Original Investigation

Characterization of Urinary Stone Composition by Use of Whole-body, Photon-counting Detector CT

Andrea Ferrero, PhD, Ralf Gutjahr, BS, Ahmed F. Halaweish, PhD, Shuai Leng, PhD, Cynthia H. McCollough, PhD

Abbreviations

EID energy integrating detector

PCD photon-counting detector

FOV field-of-view

UA uric acid

NUA non–uric acid

$CTDI_{vol}$ volume CT dose index

CTR CT number ratio

ROC receiver operating characteristic

AUC area under the ROC curve

Rational and Objectives: This study aims to investigate the performance of a whole-body, photon-counting detector (PCD) computed tomography (CT) system in differentiating urinary stone composition.

Materials and Methods: Eighty-seven human urinary stones with pure mineral composition were placed in four anthropomorphic water phantoms (35–50 cm lateral dimension) and scanned on a PCD-CT system at 100, 120, and 140 kV. For each phantom size, tube current was selected to match $CTDI_{vol}$ (volume CT dose index) to our clinical practice. Energy thresholds at [25, 65], [25, 70], and [25, 75] keV for 100, 120, and 140 kV, respectively, were used to generate dual-energy images. Each stone was automatically segmented using in-house software; CT number ratios were calculated and used to differentiate stone types in a receiver operating characteristic (ROC) analysis. A comparison with second- and third-generation dual-source, dual-energy CT scanners with conventional energy integrating detectors (EIDs) was performed under matching conditions.

Results: For all investigated settings and smaller phantoms, perfect separation between uric acid and non–uric acid stones was achieved (area under the ROC curve [AUC] = 1). For smaller phantoms, performance in differentiation of calcium oxalate and apatite stones was also similar between the three scanners: for the 35-cm phantom size, AUC values of 0.76, 0.79, and 0.80 were recorded for the second- and third-generation EID-CT and for the PCD-CT, respectively. For larger phantoms, PCD-CT and the third-generation EID-CT outperformed the second-generation EID-CT for both differentiation tasks: for a 50-cm phantom size and a uric acid/non–uric acid differentiating task, AUC values of 0.63, 0.95, and 0.99 were recorded for the second- and third-generation EID-CT and for the PCD-CT, respectively.

Conclusion: PCD-CT provides comparable performance to state-of-the-art EID-CT in differentiating urinary stone composition.

Key Words: CT; photon-counting detector CT; spectral separation; urinary stones.

INTRODUCTION

Conventional x-ray computed tomography (CT) systems rely on energy integrating detectors (EIDs), which generate an output signal that is proportional to the amount of energy deposited by the detected x-ray. Therefore, EID-CT systems inherently penalize the contribution of low-energy x-ray photons, which are the photons that carry the most contrast information for biological tissues and contrast media.

In recent years, a number of preclinical photon-counting detector (PCD) CT systems were introduced (1–3). Unlike EID-CT, PCD-CT systems directly convert each detected x-ray photon into individual pulses with amplitudes proportional to the energy of the incoming photon. Each individual pulse is counted separately through the use of fast electronics. The equal contribution of each detected photon regardless of their energy (4,5), combined with a reduced influence of electronic noise, results in improved contrast-to-noise ratio for PCD-CT when compared to EID-CT techniques (6). Additionally, PCD-CT can provide acquisitions with full field-of-view (FOV), fully registered data, stability against motion artifacts, no cross scatter from a second x-ray tube, and the ability to configure more than two energy thresholds. Finally, all measurements provide multienergy information,

Acad Radiol 2018; ■:■■–■■

From the Department of Radiology, Mayo Clinic, 200 First Street SW, Rochester, MN 55905 (A.F., S.L., C.H.MC.); Institut für Informatik, Technische Universität München, Garching bei München, Germany (R.G.); Siemens Healthcare, Malvern, Pennsylvania (A.F.H.). Received June 23, 2017; revised January 2, 2018; accepted January 2, 2018. Funding Sources: The project described was supported by grant number DK100227 from the National Institute of Diabetes and Digestive and Kidney Diseases and grant numbers EB016966 and RR018898 from the National Institute of Biomedical Imaging and Bioengineering of the National Institutes of Health. The content is solely the responsibility of the authors and does not necessarily represent the official views of the National Institutes of Health. **Address correspondence to:** C.H.M. e-mail: mccollough.cynthia@mayo.edu

https://doi.org/10.1016/j.acra.2018.01.007

enabling the application of dual-energy or multienergy post-processing algorithms for every scan.

The system utilized in this study is a whole-body PCD-CT research system (SOMATOM CounT; Siemens Healthcare, Forchheim, Germany) (7–9). Preliminary in vivo animal and human studies demonstrated its ability to provide CT images of diagnostic quality for several applications, including unenhanced and iodine-enhanced abdominal imaging (10,11).

Renal stone characterization has been one of the most established clinical applications of dual-energy CT to date. Current state-of-the-art dual-energy CT systems can noninvasively separate uric acid (UA) from non–uric acid (NUA) stones, with near 100% accuracy at the same radiation dose as routine, single-energy renal stone CT examinations, providing valuable information to the ordering physician to guide treatment options (12). Therefore, in this work, we characterized ex vivo the performance of a PCD-CT system in differentiating the mineral composition of urinary stones and compared it to two commercial dual-energy EID-CT systems. As one of the potential advantages of PCD-CT is the ability to add spectral information to any CT examination and since low-tube potential imaging is a popular and effective method to reduce radiation dose, especially in contrast-enhanced abdominal CT scans, we extended the characterization to lower tube potential.

MATERIALS AND METHODS

Institutional Review Board protocol approval was not required for this nonpatient study. However, biospecimen approval was obtained from the institutional biospecimen committee.

Stone Samples

A set of 87 urinary stones was investigated, including UA ($n = 17$), cystine ($n = 5$), calcium oxalate ($n = 30$), brushite ($n = 5$), and apatite ($n = 30$). Reference composition was given by micro-CT and infrared spectroscopy (13). Only stones with purity higher than 90% were included in the cohort, with one stone sample selected from each individual patient. The stones were hydrated for 24 hours before being embedded in gelatin in two 60-well ice cube trays and placed in four torso-shaped water tanks with lateral dimensions of 35, 40, 45, and 50 cm, which were used to represent small, average, large, and obese adults, respectively. Figure 1 shows the experimental setup.

PCD-CT Data Acquisition and Reconstruction

All phantoms were scanned on a whole-body, PCD-CT research system. Three different tube potentials were investigated: 100, 120, and 140 kVp. For each tube potential, the threshold that resulted in the most uniform distributions of the detected x-rays between the low and high bin was selected. Figure 2 shows the detected energy spectra for the three settings used.

As the scanned objects exceeded the 275-mm FOV of the PCD subsystem, a data-completion scan from the EID subsystem (500-mm FOV) was used to obtain artifact-free images. This additional scan has been shown to be successfully performed using very low radiation doses (14). For each phantom size, the tube output was selected to match the volume CT dose index ($CTDI_{vol}$) to our clinical practice. Table 1 summarizes the PCD-CT acquisition parameters used for all scans.

Dual-energy PCD-CT data were obtained whereby the low-energy image included x-rays with energies between the two detector thresholds (eg, 25–65 keV), and the high-energy image included x-rays with energies above the higher detector energy threshold (eg, 65–100 keV). All images were reconstructed using the protocol parameters adopted in our clinical practice for renal stone composition: weighted filtered-backprojection reconstruction, 275-mm FOV, 1.0-mm thick slices with 0.8-mm slice interval, and a medium-sharp soft-tissue D30f reconstruction kernel.

Image Processing and Classification Analysis

Kidney stones were automatically segmented using previously validated in-house software (15). Metrics describing

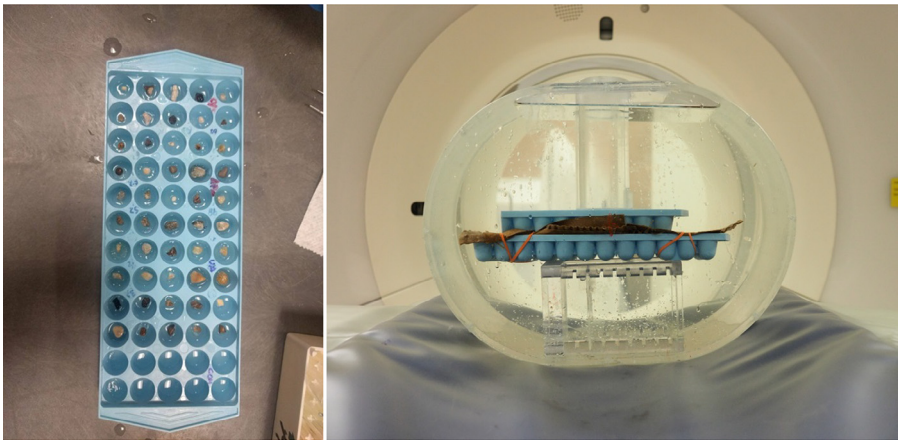

Figure 1. Experimental setup.